PERGAMON

Solid State Communications 112 (1999) 587–591

solid state communications

www.elsevier.com/locate/ssc

Pair correlation in two-electron emission from surfaces

J. Berakdar[a,*], H. Gollisch[b], R. Feder[b]

[a]*Max-Planck-Institut für Mikrostrukturphysik, Weinberg 2, 06120 Halle, Germany*
[b]*Theoretische Festkörperphysik, Universität Duisburg, D-47048 Duisburg, Germany*

Received 23 July 1999; accepted 28 July 1999 by P. Dederichs

Abstract

An electron pair emitted from a crystalline surface system is represented by a relativistic two-electron scattering state, which contains the pair correlation mediated by a screened Coulomb interaction. This state is obtained from the solutions of two one-electron Dirac equations with potentials, which incorporate the electron–electron interaction as a dynamical screening of the usual effective one-electron potentials. Numerical applications to the electron pair emission due to low-energy electron impact on a He atom and on a clean W(001) surface demonstrate that pair correlation effects can be quite strong and significantly improve the agreement of calculated results with experimental data.

Keywords: A. Metals; A. Surfaces and interfaces; D. Electron–electron interactions; E. Electron emission spectroscopies

The simultaneous two-electron emission induced by electron impact on atomic and solid targets, so-called (e,2e) spectroscopy, has a long history of success for high-energy primary electrons (cf. e.g. [1–3] and references therein). For low-energy primary electrons (with less than a few 100 eV) impinging on a crystalline surface and momentum-resolved pair observation in the reflection mode, substantial experimental and theoretical progress was made only fairly recently [4–10]. Good overall agreement between experimental data and their calculated counterparts was achieved and details of the (e,2e) mechanism were thence revealed.

In the existing theoretical treatments (cf. [6,8,9]), the two ejected electrons are described by an anti-symmetrized product of single-particle states. Whilst a "pair correlation" due to exchange (Pauli principle) is thus incorporated, the Coulomb interaction between the two ejected electrons has not been taken into account. On the other hand, the Coulomb pair correlation is known to be vital for photon-induced two-electron emission [11,12]. We therefore explore in the present work its potential importance in the low-energy (e,2e) process by formulating a theoretical method and applying it numerically to the prototype surface W(001).

To incorporate the Coulomb interaction between the two ejected electrons, at least, an effective "quasi *two*-particle" theory is needed. The initial asymptotic state of the system is an anti-symmetrized direct product of two single quasi-particle states, which represent the projectile electron and an individual valence electron, i.e. $|1,2\rangle = |1\rangle \otimes |2\rangle$. The states $|1\rangle$ and $|2\rangle$ are solutions of a Dirac equation involving optical potentials V_1 and V_2, respectively, which incorporate the interaction with the nuclei and all the other ground state electrons. We recall (cf. e.g. [9]) that for a semi-infinite crystalline system with lattice periodicity parallel to the surface relativistic one-electron states $|i\rangle$ are characterized by energies, E_i, surface-parallel two-dimensional wave vectors $\mathbf{k}_i^{\parallel}$ and spin labels σ_i. The number i in $|i\rangle$ is thus an abbreviation for the set of quantum numbers $(E_i, \mathbf{k}_i^{\parallel}, \sigma_i)$. For the relativistic LEED (low energy electron diffraction) state $|1\rangle$, the set $(E_1, \mathbf{k}_1^{\parallel}, \sigma_1)$ is dictated by the experimental conditions and is equivalent to the three-dimensional wave vector $\mathbf{k}_1$ and the spin alignment at the electron gun. Even if the primary beam is unpolarized, states $|1\rangle$ with $\sigma_1 = \pm$ have to be employed and finally summed over. The same holds in any case for the valence states $|2\rangle$.

For the electron–electron interaction U considered as a perturbation, standard scattering theory gives the transition amplitude for the initial state $|1,2\rangle$ to go over into the two-electron excited state $|3,4\rangle$ as

$$W(1,2;3,4) = \langle 3,4|U|1,2\rangle. \quad (1)$$

* Corresponding author. Fax: + 49-345-55-11223.
E-mail address: jber@mpi-halle.de (J. Berakdar)

0038-1098/99/$ - see front matter
PII: S0038-1098(99)00365-8

Strictly speaking, $|3,4\rangle$ is an eigenstate of a two-electron Dirac equation involving the total potential

$$V_{\rm tot} = V_3 + V_4 + U, \tag{2}$$

where V_3 and V_4 are one-particle optical potentials, and with asymptotic boundary conditions such that an electron with momentum $\mathbf{k}_3$ and spin alignment σ_3 arrives at one detector and an electron with momentum $\mathbf{k}_4$ and spin alignment σ_4 at the other detector. Obviously, an exact solution of this non-separable many-body equation is not possible. On the other hand, if we neglect in Eq. (2) the interaction term U, the state $|3,4\rangle$ reduces to an anti-symmetrized direct product of two independent time-reversed LEED states, $|3\rangle$ and $|4\rangle$, as was done in previous work [8,9]. Since these (uncoupled) LEED states $|3\rangle$ and $|4\rangle$ are calculated using one-particle optical potentials V_3 and V_4, respectively, each of them contains—within the framework of a local spin density approximation to exchange and correlation terms—the exchange and correlation with all the other "passive electrons".

The interaction U between the two active electrons must be included in a dynamic way that reflects the dependence of the mutual coupling on the electrons' positions relative to each other. For example, the interaction between the two electrons is strongest when they escape close to each other, whereas this interaction diminishes when the electrons are far apart.

To implement this dynamical coupling, we first identify the electron pair interaction U as a Coulomb potential, which is screened by the ground state electrons of the semi-infinite crystal. Since the calculation of a realistic dielectric function $\epsilon(\mathbf{r},\mathbf{r}')$ for such a highly inhomogeneous electron gas is beyond the scope of this work, we adopt the Thomas–Fermi form $U(\mathbf{r}_3,\mathbf{r}_4) = \exp(-r_{34}/\lambda)/r_{34}$, where $\mathbf{r}_3$ and $\mathbf{r}_4$ are the positions of the two active electrons and $\mathbf{r}_{34} = \mathbf{r}_3 - \mathbf{r}_4$. To obtain a physically reasonable estimate of the screening length, λ, we start from the Thomas–Fermi expression (at $T = 0$) $\lambda = (4\pi e^2 N(E_{\rm F}))^{(-1/2)}$, where $N(E_{\rm F})$ is the total density of states at the Fermi energy $E_{\rm F}$. Rather than approximating $N(E_{\rm F})$ by a non-interacting homogeneous electron gas value, as is frequently done, we take it from a self-consistent electronic structure calculation for the actual crystal. Employing the simple Thomas–Fermi form appears reasonable in this work, firstly because it is our aim to get first and perhaps only semi-quantitative results on pair correlation effects, and secondly, because it led to rather good agreement between theory and experiment in a recent (e,2e) study on W(001) [9].

With this approximation for U, we return to the potential $V_{\rm tot}$ (Eq. (2)). We express the one-electron potentials V_3 and V_4 as lattice sums over potentials w_3 and w_4 residing in muffin tin spheres around the lattice sites. Inside each sphere, we then have the total potential $W_{\rm tot} = w_3 + w_4 + U$. With the above Thomas–Fermi expression for U, this can easily be reformulated as

$$W_{\rm tot} = w_3 + \frac{Z_3}{r_3} + w_4 + \frac{Z_4}{r_4} \tag{3}$$

where

$$Z_j = a_j^{-1} \exp\left(-\frac{a_j}{2\lambda} r_j\right), \qquad j = 3,4, \tag{4}$$

with $a_j = 2r_{34}/r_j$. The interpretation of Eq. (3) is straightforward. Owing to the electronic correlation, the single-particle potentials w_j, $j = 3,4$ are augmented by the term Z_j/r_j. This means that the inter-electronic correlation is subsumed into a dynamic non-local screening of the electron core interaction.

The strength of this screening is determined by the functions Z_j, as given by Eq. (4). In fact, the augmented electron core potentials $\bar{w}_j = w_j + Z_j/r_j$ may even turn repulsive when the two electrons are "on top of each other" ($r_{34} \to 0$).. If the two electrons are far away from each other ($r_i \gg r_j$, $i \neq j \in [3,4]$) the screening strengths Z_3 and Z_4 become negligible and we end up with two independent particles ($\bar{w}_j \to w_j$). Furthermore, if one of the electrons approaches closely the ionic sites its motion becomes dominated by the corresponding ionic potential w_j. This is readily deduced from the relation $\lim_{r_j \to 0} \bar{w}_j \to w_j$.

Our dynamic screening expression in Eq. (3) is, for the above-defined U, merely a rearrangement of the interaction terms in Eq. (2). Its direct numerical implementation is extremely difficult. In the present exploratory study, we therefore approximate the dynamical screening strengths Z_j by $\bar{Z}_j = \bar{a}_j^{-1} \exp(-(\bar{a}_j/2\lambda) r_j)$ with $\bar{a}_3 = 2v_{34}/v_3$ and $\bar{a}_4 = 2v_{34}/v_4$, where $\mathbf{v}_3$ and $\mathbf{v}_4$ are velocities of the two emitted electrons and $\mathbf{v}_{34} = \mathbf{v}_3 - \mathbf{v}_4$. The approximation $\bar{Z}_j \approx Z_j$ amounts to assuming $\mathbf{r}_3 \propto \mathbf{v}_3$ and $\mathbf{r}_4 \propto \mathbf{v}_4$; this means that the potential Eq. (2) is exactly diagonalized when the particles proceed along trajectories where the positions are proportional to the velocities. Whilst inside the solid this is of course not the case, we feel that the above approximation is of a semi-quantitative value if we choose the two velocities $\mathbf{v}_i = \mathbf{k}'_{i0}/m$—with $i = 3,4$—where $\mathbf{k}'_{i0}$ is the wave vector of the 00 LEED beam inside the crystal, which is obtained from the wave vector $\mathbf{k}_{i0}$ outside the crystal (and in particular at the detector) by refraction at the surface potential barrier.

To assess the quality of the above approach we evaluate at first the amplitude Eq. (1) for an atomic helium target in its ground state. This should give a direct insight into the single-site behavior of the dynamic screening. In this case the states $|3(\bar{Z}_3(\mathbf{v}_3,\mathbf{v}_4))\rangle$ and $|4(\bar{Z}_4(\mathbf{v}_3,\mathbf{v}_4))\rangle$ are derived from the corresponding Schrödinger equation for one particle moving in the electrostatic field of He^+ with an effective screening of this field given by $\bar{Z}_j(\mathbf{v}_3,\mathbf{v}_4)$, $j = 3,4$. The electron–electron interaction is assumed unscreened, i.e. $\lambda \to \infty$. The cross-section with appropriate flux normalization is readily obtained from the transition amplitude, Eq. (1) [6]. Fig. 1 shows the cross-section at 2 eV above the single

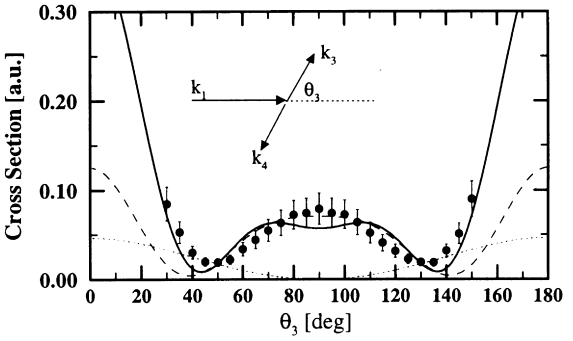

Fig. 1. The cross-section for the emission of two equal-energy electrons following the collision of an electron with an atomic He($^1S^e$) target. The excess energy of the pair is 2 eV. The angular correlation pattern is depicted as a function of the angle of the interelectronic axis with respect to the beam direction (see inset). The calculations with (continuous line) and without (dashed curve) dynamical screening are shown along with the results of the first Born approximation (dotted line) (see text for more details). The experimental data are taken from Ref. [14] where comparison with other theoretical methods can be found.

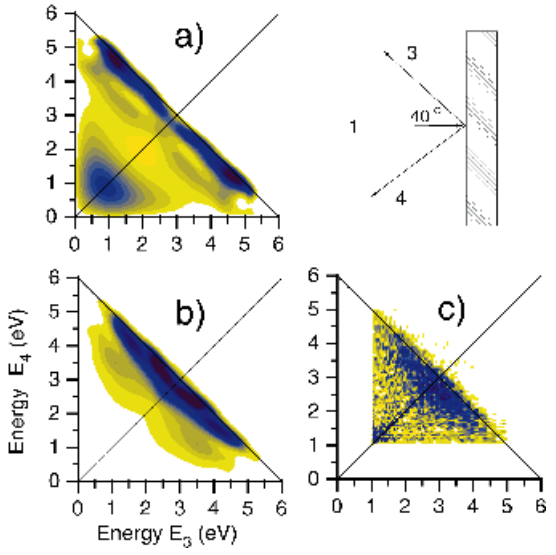

Fig. 2. Spin-averaged intensity for the two-electron emission from a W(001) surface following the impact of a 10.6 eV electron along the surface normal (chosen as the z-axis), i.e. polar angle of incidence $\theta_1 = 0$. The direction [100] defines the x axis. The emitted electrons are detected in the x–z plane, i.e. their azimuthal angles are $\phi_3 = 0$ and $\phi_4 = 180°$, and the polar angles are set to $\theta_3 = \theta_4 = 40°$. The contour plots in the (E_3,E_4)-plane show calculated results without Coulomb pair correlation (panel a) and with pair correlation according to Eq. (3) (panel b), in comparison with experimental data (panel c) [15]. For outgoing pair energies indicated by the solid counter-diagonal lines, the corresponding valence electron energy is the Fermi energy. Along the diagonal lines, the two outgoing electrons have equal energies.

ionization threshold of He as a function of the interelectronic axis with respect to the incident beam direction. As shown in the inset, both electrons escape with the same energy (1 eV) and opposite to each other, i.e. $\hat{\mathbf{k}}_3 \cdot \hat{\mathbf{k}}_4 = -1$. The absolute experimental data are well reproduced by the present theory. To highlight the effect of correlation we also show in Fig. 1 the results neglecting the dynamic screening, i.e. we discard U in Eq. (2). This leads to results clearly at variance with the experimental finding. Furthermore, the importance of the coupling to the ionic core can be demonstrated by switching off U and V_3, i.e. one electron moves in the field of the residual ion whereas the second one is considered as free. This inadequate (cf. Fig. 1) procedure amounts to the well-known first Born approximation. The geometry depicted in Fig. 1 is in so far remarkable as in this situation the electronic correlation is minimal (at fixed total excess energy of 2 eV). Thus for situations where the electrons are detected close to each other in velocity space we can expect an even more striking effect of the pair correlation.

Having established the usefulness of the above method for single-site reactions we turn now to its application to (e,2e) spectroscopy from the clean crystal surface W(001), which was recently studied in detail experimentally and by calculations without the Coulomb pair correlation [9]. Employing a relativistic layer-KKR method [13] we numerically calculate the correlated time-reversed LEED states $\langle 3(\bar{Z}_1(\mathbf{v}_3, \mathbf{v}_4))|$ and $\langle 4(\bar{Z}_2(\mathbf{v}_3, \mathbf{v}_4))|$, each of which depends on the velocities $\mathbf{v}_3$ and $\mathbf{v}_4$ of the *two* electrons—chosen above as velocities of the 00 LEED beams inside the crystal—and their mutual relative velocity. For the screening length λ of the electron–electron interaction (cf. earlier) we obtained, with the aid of a self-consistent LMTO calculation for W, the value $\lambda = 0.48$ Å. The cross-section is then calculated as in [9]. It essentially involves absolute squares of transition amplitudes (cf. Eq. (1)) summed over all spin labels σ_i (with $i = 1, \ldots, 4$), since we wish to make contact with experiments without any spin resolution.

For the experimental conditions used in [9]—with primary electron energies between 16 and 24 eV and an angle of 80° between the directions of the two outgoing electrons—we find only rather small pair correlation effects, and the fairly good agreement between experiment and theory, which was reached in [9], remains practically unchanged. For different conditions, however, quite drastic effects emerge.

Firstly, we retained the coplanar geometry with the large angle between the two detected electrons, but lowered the primary energy to 10.6 eV, which implies a maximal total energy of the pair of 6 eV. The intensity distribution calculated without Coulomb pair correlation, i.e. for $Z_3 = 0 = Z_4$ in Eq. (3), is shown in Fig. 2a. For total pair energies between 5 and 6 eV, the intensity is small for $E_3 = E_4$ and has maxima around $(E_3, E_4) = (4.8, 1.0)$ and (1.0,4.8). In contrast, the spectra obtained with pair correlation (Fig. 2b) are maximal closer to and around $E_3 = E_4$. This is

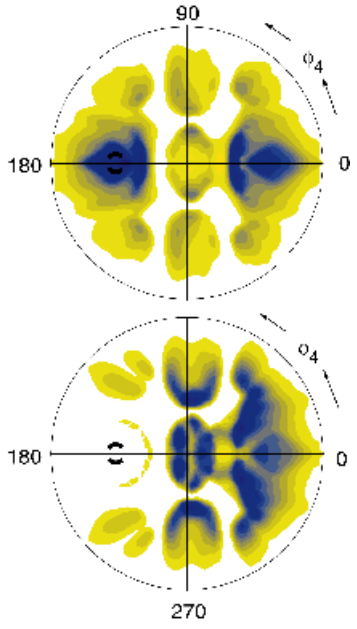

Fig. 3. Calculated spin-averaged angular distributions of two electrons emitted from W(001) upon impact of electrons with primary energy 17.2 eV. The polar and azimuthal angles of the incident electron are $\theta_1 = 88°$ (i.e. grazing incidence) and $\phi_1 = 0°$. The two outgoing electrons are detected with equal energies $E_3 = E_4 = 6$ eV. One electron detector is fixed at a direction defined by $\theta_3 = 47°$ and $\phi_3 = 180°$. The coincident emission rate is scanned as a function of the angles θ_4 and ϕ_4 of the other electron detector, which correspond to the radial and angular coordinates in the contour plots. The Coulomb pair correlation between the two outgoing electrons is switched off in the upper panel and taken into account according to Eq. (3) in the lower panel. The broken circle around $\theta_4 = 47°$ and $\phi_4 = 180°$ marks the direction of parallel escape of the two electrons, i.e. the centre of the "pair correlation hole".

understandable from the fact that the Coulomb interaction can transfer energy from the one escaping electron to the other. Close to the threshold, around $(E_3, E_4) = (1, 1)$, where refraction implies a very small angle between $\mathbf{v}_3$ and $\mathbf{v}_4$, the electron–electron interaction is seen to prevent pair emission. Comparison with experimental data [15] (cf. Fig. 2c) shows that the inclusion of pair correlation significantly improves the agreement for total pair energies between 4 and 6 eV. As for the intensity around $(E_3, E_4) = (1, 1)$, we recall from [9] that this feature in experimental data is likely to arise from two accidentally time-correlated secondary electrons. Altogether, our calculations predict a strong influence of the pair correlation, which is substantiated by experimental findings.

The dependence of correlation effects on the angle between the two outgoing electrons is demonstrated in Fig. 3, where the detection direction of one electron is fixed and that of the other sweeps over the entire hemisphere. Comparison of the calculated results in the upper half of Fig. 3 with those in the lower half shows that the inter-electronic coupling results in a drastic modification of the angular distribution pattern. Without correlation, the emission probability is seen (cf. upper half of Fig. 3) to be maximal when the two electrons escape into the same direction and with the same velocity. This unphysical result is remedied by the pair interaction (cf. lower half of Fig. 3), which carves a considerable "pair correlation hole" around the position where electrons are close to each other in velocity space. For regions where the two electrons emerge with diverging directions, the effect of the pair correlation becomes less and less visible.

In conclusion, we have presented a theoretical formalism for including the Coulomb pair correlation in the calculation of *two-electron* scattering states from single atoms and from crystalline surface systems. This has been achieved through position-dependent dynamical screening of the usual effective one-electron potentials. For the actual evaluation of transition amplitudes, the position dependence has been approximated by a velocity dependence. Numerical results for an atomic target and for a crystal surface demonstrate that pair correlation effects can be important in two-electron emission upon low-energy electron impact. The application of the present formalism to electron pair emission due to the absorption of a VUV photon [11], a reaction forbidden in the absence of the pair correlation [12], is currently in progress.

Acknowledgements

We would like to thank S.N. Samarin for making available the experimental data shown in Fig. 2c.

References

[1] I.E. McCarthy, E. Weigold, Rep. Prog. Phys. 54 (1991) 789.
[2] M. Vos, I.E. McCarthy, Rev. Mod. Phys. 67 (1995) 713.
[3] C.T. Whelan, H.R.J. Walters (Eds.), Electron Coincidence Studies of Electron and Photon Impact Ionization Plenum, New York, 1997.
[4] J. Kirschner, O.M. Artamonov, S.N. Samarin, Phys. Rev. Lett. 75 (1995) 2424.
[5] O.M. Artamonov, S.N. Samarin, J. Kirschner, Appl. Phys. A 65 (1997) 535.
[6] J. Berakdar, M.P. Das, Phys. Rev. A. 56 (1997) 1403.
[7] J. Berakdar, S.N. Samarin, R. Herrmann, J. Kirschner, Phys. Rev. Lett. 81 (1988) 3535.
[8] H. Gollisch, G. Meinert, Xiao Yi, R. Feder, Solid State Commun. 102 (1997) 317.
[9] R. Feder, H. Gollisch, D. Meinert, T. Scheunemann, O.M. Artamonov, S.N. Samarin, J. Kirschner, Phys. Rev. B 58 (1998) 16418.
[10] A.S. Kheifets, S. Iacobucci, A. Ruoccoa, R. Camilloni, G. Stefani, Phys. Rev. B 57 (1998) 7380.

[11] R. Herrmann, S.N. Samarin, H. Schwabe, J. Kirschner, Phys. Rev. Lett. 81 (1998) 2148.
[12] J. Berakdar, Phys. Rev. B 58 (1908) 9808.
[13] R. Feder (Ed.), Polarized Electrons in Surface Physics World Scientific, Singapore, 1985.
[14] T. Rösel, J. Röder, L. Frost, K. Jung, H. Ehrhardt, S. Jones, D.H. Madison, Phys. Rev. A 46 (1992) 2539.
[15] S.N. Samarin, private communication.